



## Investigation of white layer thickness, material removal rate, and tool wear rate of Inconel 718 by nano- $\text{Al}_2\text{O}_3$ -mixed electrical discharge machining



Dunya A. Ghulam\* , Abbas F. Ibrahim 

Production Engineering and Metallurgy Dept., University of Technology-Iraq, Alsina'a street, 10066 Baghdad, Iraq.

\*Corresponding author Email: [dunia.a.ghulam@gmail.com](mailto:dunia.a.ghulam@gmail.com)

### HIGHLIGHTS

- NPMEDM performance was enhanced with a magnetic field and Nano  $\text{Al}_2\text{O}_3$  in soybean oil.
- The current, pulse-on-time, powder concentration, and magnetic field effects on WLT, MRR, and TWR were analyzed.
- WLT was decreased by 54.32%, MRR was increased by about 42.193%, and TWR was reduced by 80.44%.
- Current and powder concentrations were the most influential parameters on NPMEDM performance.

### ARTICLE INFO

**Handling editor:** Omar H. Hassoon

**Keywords:**

NPMEDM; Nano  $\text{Al}_2\text{O}_3$ ; Inconel 718 alloy; WLT; MRR.

### ABSTRACT

Nano powder mixed electrical discharge machining (NPMEDM) is an advanced thermo-physical process. It is used to create complex, precise shapes in hard-to-machine materials, such as nickel-based alloys like Inconel 718, due to their mechanical properties. This study introduces magnetic field assistance to improve the discharge state. Nano aluminum oxide was added to biodegradable soybean oil, serving as the insulating fluid to machine Inconel 718 alloy. The study examined the impact of machining parameters, including current, pulse on time, powder concentration, and magnetic field assistance, on outcomes like white layer thickness, material removal rate, and tool wear rate. Minitab software facilitated a general full factorial multi-level design to analyze the results. Findings showed that adding nano  $\text{Al}_2\text{O}_3$  with a magnetic field is crucial in enhancing process performance. The lowest white layer thickness achieved was 20.59  $\mu\text{m}$ , showing a 54.32% improvement. The highest material removal rate was 13.259  $\text{mm}^3/\text{min}$ , with an increase of 42.193%. The tool wear rate also improved; the minimum value was 0.0228  $\text{mm}^3/\text{min}$ , reduced by about 80.44% compared to using no powder in the dielectric fluid. Optimal settings to enhance performance were found to be a current of 8 A, pulse on time of 100  $\mu\text{s}$ , powder concentration of 4 g/l, and a magnetic field intensity of 0.2 T.

## 1. Introduction

One of the non-conventional machining techniques is electro-discharge machining (EDM); it can be used to machine metals that are impractical and difficult to machine using conventional Techniques [1]. In the EDM process, material removal occurs due to the spark discharge in the machining gap between the machined surface and the used electrode [2]. A very high elevated temperature (8000 to 12000 °C) generated in the machining gap due to the electrical discharge results in the melting and vaporizing of the machined material; material removal happens [3]. Different medical, aerospace, and automotive industries have widely adopted EDM to produce high-precision elements and parts [4]. Several techniques have been developed to improve this important process, including adding powders to the used insulating fluid called powder mixed electrical discharge machining (PMEDM). When powder is added to the insulating fluid, the material removal rate, surface quality, and white layer thickness will improve [5]. Through a literature survey, it was noted that several researchers studied the effect of adding different kinds of powders to the insulating fluid. Tiwarya et al. [6], reported that when adding powders, the insulating strength of the dielectric is reduced, and the gap distance between the tool and the machined surface increases, hence the removal of molten material from the machining gap is efficiently and uniformly; thus, the process improves. Bhattacharya et al. [7], mentioned that transferring added powder particles to the machined surface will change its chemical composition and produce in-demand improvements for the machined surface. Mughal et al. [8], modified the surface of the medical-grade titanium  $\alpha + \beta$  ELI alloy by mixing SiC with the insulating fluid. The results showed that the machined surface's surface roughness and fracture density were reduced significantly at 20 g/l of SiC concentration. Farooq et al. [9], investigated the surface integrity of Ti6Al4V by adding Si to the kerosene dielectric. Findings observed that a five g/l concentration of Si

was the optimum parameter that produced 13.8  $\mu\text{m}$  thickness of the white layer and 2.76  $\mu\text{m}$  surface roughness. Ibrahim [10], investigated the influence of adding  $\text{Al}_2\text{O}_3$  to the dielectric on MRR and SR to machine AISI 304 stainless steel. The results determined the appropriate parameters for machine AISI 304. MangapathiRao et al. [11], mixed nano  $\text{Al}_2\text{O}_3$  with sunflower oil to machine AISI D2 steel. The experimental results observed that minimum surface roughness, a higher material removal rate, and a lower tool wear rate were produced after adding nano  $\text{Al}_2\text{O}_3$  to sunflower oil. Tawfig and Hameed [12], studied the influence of aluminum, manganese, and aluminum-manganese mixing with different concentrations to machine several kinds of die steel. The results indicate that manganese considerably affects MRR. Further, nickel-based alloys like Inconel 718 are difficult to machine by conventional techniques due to their mechanical properties, among other nontraditional techniques; PMEDM is a convenient process for machining nickel-based alloys [13]. Many researchers studied Inconel machining by PMEDM, like Paswan et al. [14] where the influence of aluminum powder addition to the dielectric was studied. MRR in PMEDM was higher than conventional EDM, as reported in this study the machining performance of PMEDM, which is used to machine Inconel 718, was improved using graphene nanofluid. During the comparison between EDM and NPMEDM to machine Inconel, by adding nano  $\text{Al}_2\text{O}_3$  to the dielectric, it was confirmed that NPMEDM has better surface quality and a higher MRR than traditional EDM [15].

Kumar et al. [16], investigated the performance of EDM by adding nano  $\text{Al}_2\text{O}_3$  to deionized water to machine Inconel 825. The experimental results conducted that the MRR improved by 44%, and the Ra improved by 51% as compared to traditional EDM performance. On the other hand, one of the issues in the PMEDM process is removing debris from the machining gap; a magnetic field assistance strategy was developed to overcome this issue. Using MF improves machining stability by increasing the rate of stable discharge [17]. Furthermore, the problem of powder particles accumulation in the machining tank due to its density was solved by adding surfactant to the dielectric with a suitable concentration. As a result, process performance improved due to the stability of the process [18]. Reviewing the previous research, it became clear that the number of studies on machining Inconel 718 using the magnetic field assistance technique with the addition of nano  $\text{Al}_2\text{O}_3$  powder are rare and need more investigation. The present research studied the effect of the magnetic field and the effect of adding nano  $\text{Al}_2\text{O}_3$ . Nano  $\text{Al}_2\text{O}_3$  was chosen because of its high thermal conductivity and was added to a biodegradable insulating fluid to enhance EDM process performance to machine Inconel 718 alloy. Experiments were carried out and analyzed using a general complete factorial multi-level design at different current conditions, pulse on time, powder concentration, and magnetic field to observe their impact on WLT, MRR, and TWR.

## 2. Experimental work

### 2.1 Materials

The machined workpiece was a nickel-based superalloy (Inconel 718). The NPMEDM process was used to machine it because it is hard to machine by conventional processes due to its high ultimate tensile strength, which is between 800 and 1300 MPa, and its modulus of elasticity is 200 GPa. The melting point is about 1260 and 1335  $^{\circ}\text{C}$ . The workpieces' dimensions were 25 $\times$ 10 $\times$ 4 mm. Copper was chosen as an electrode tool due to its high electrical conductivity and melting point 1083.4  $^{\circ}\text{C}$ . Turning and milling machines were used to fabricate the electrodes to the required dimensions and shapes 15 $\times$ 10 $\times$ 70 mm. The added powder was nano  $\text{Al}_2\text{O}_3$  (see Figure 1), whose thermal conductivity is 32 W/m.K, its density is 3.95  $\text{g}/\text{cm}^3$ , and its melting point is 2072  $^{\circ}\text{C}$ . The average particle size of nano  $\text{Al}_2\text{O}_3$  was 30 nm. Soybean oil is an insulating fluid; it is non-toxic, biodegradable, and renewable. It has a lower impact on the environment. Considering the need for the nano  $\text{Al}_2\text{O}_3$  powder particles to remain suspended in the dielectric fluid, Tween 60 was used as a surfactant. To help improve machining performance, two pieces of permanent magnets were used; their types were neodymium (NdFeB) magnets, and the produced intensity of the magnetic field was 0.2 T.

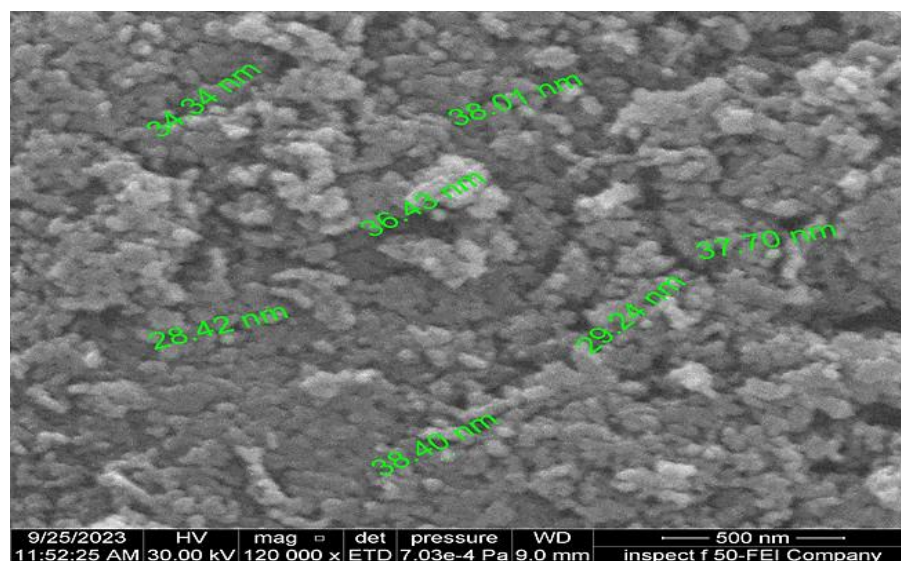


Figure 1: SEM for nano  $\text{Al}_2\text{O}_3$  powder particles

### 2.2 Experimental setup

The practical experiments were implemented using the electrical discharge machine model CHMER EDM (50N). The machining tank was fabricated from galvanized iron; its dimensions were 500×200×250 mm as shown in Figure 2. It was supplied with a unique system to circulate the dielectric, involving a pump, flushing nozzle, and a pipe of diameter 5 mm installed along the internal walls of the machining tank; this pipe was provided with eight holes of diameter 1 mm along its expansion, thereby preventing particles from accumulating in the base of the tank and continuously moving throughout the dielectric fluid, which in turn improves process performance. Throughout the flushing nozzle, the insulating fluid containing the nanoparticles of AL<sub>2</sub>O<sub>3</sub> was pumped into the machining zone; these nanoparticles energized and contributed to the machining process improvement. The experimental setup is shown in Figure 3.

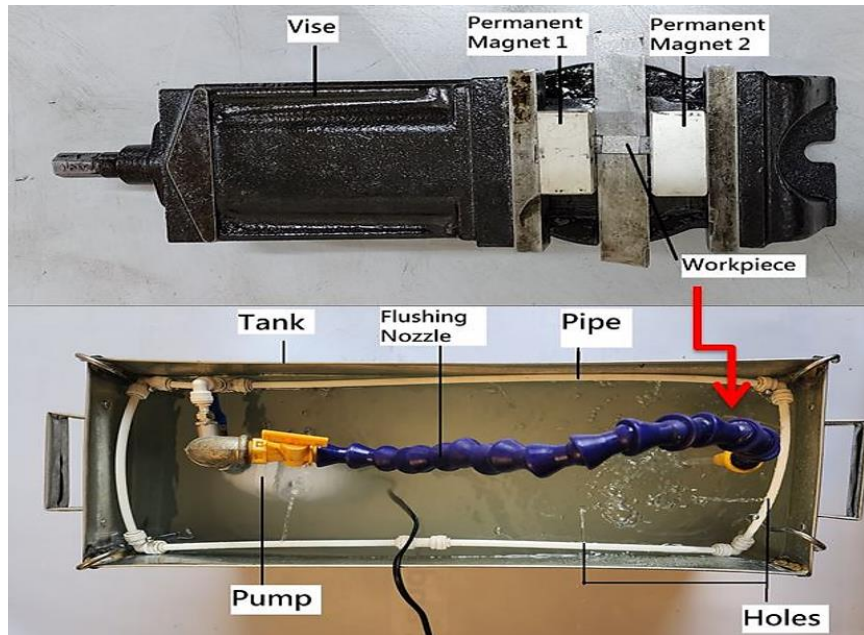


Figure 2: Machining tank

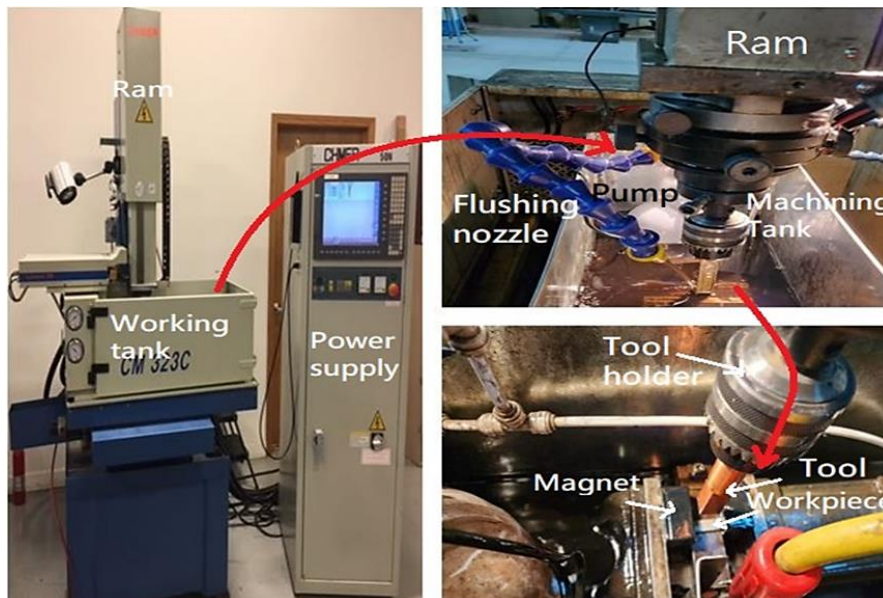


Figure 3: Experimental setup

### 2.3 Process parameters selection

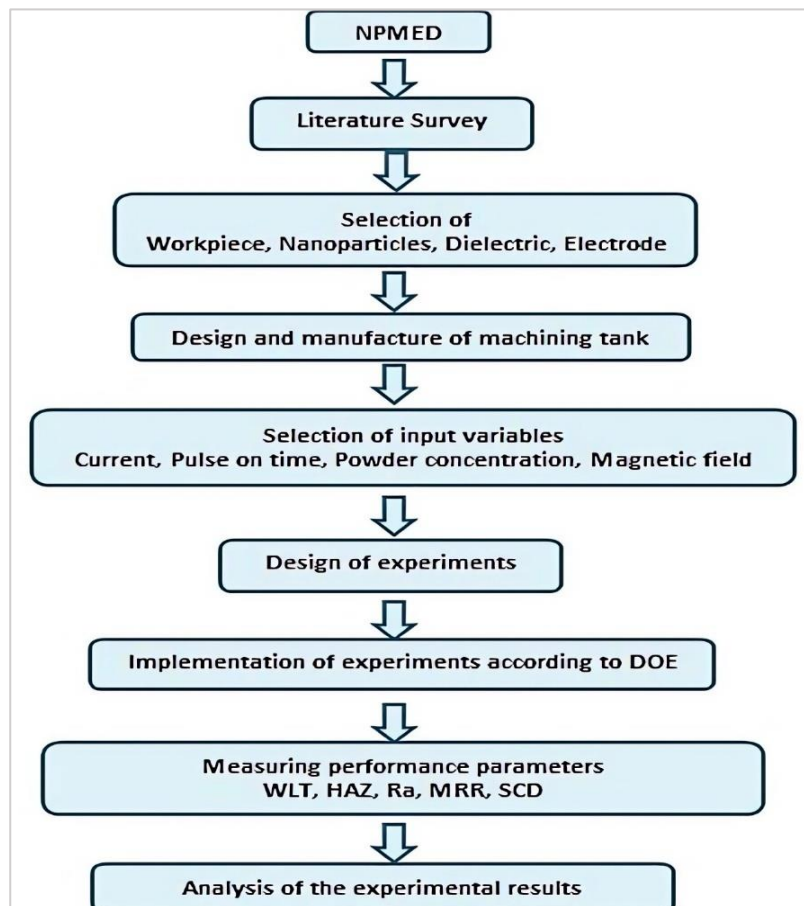
The practical experiments were designed by Minitab 2022 software using a multi-level general complete factorial design. The input parameters with different levels were current (I) A, pulse on time (Ton) μs, powder concentration (con.) g/l, and magnetic field (MF) T (see Table 1). These parameters were analyzed to see their effect on responses, which were the white layer thickness (WLT) μm, material removal rate (MRR), and tool wear rate (TWR). On the other hand, the rest of the parameter values were kept fixed during the machining process, as shown in Table 2. The flow chart of the process is shown in Figure 4.

**Table 1:** Variable parameters' levels

Parameter	Unit	Level 1	Level 2	Level 3
I	(A)	8	16	/
Ton	( $\mu$ s)	100	200	/
Con.	(g/l)	0	2	4
MF	(T)	0	0.2	/

**Table 2:** Fixed parameters'

Parameter	Value
Pulse off time (Toff)	75 ( $\mu$ s)
Powder	Al <sub>2</sub> O <sub>3</sub>
Particles size	30 (nm)
Polarity	Straight
Gap voltage	240 (V)
Surfactant type	Tween 60
Surfactant con.	1 (ml/l)
Depth of cut	1(mm)

**Figure 4:** The flow chart of the experimental work

### 3. Results and discussion

#### 3.1 Impact of machining parameters on WLT

Different microstructures are generated during the machining process due to temperature changes, which affect the properties of the white layer [19]. The white layer is an essential indicator of the machined surface hardness; it arises from the re-solidification of the molten metal during the machining process. The thickness of the white layer is affected by powder additions to the dielectric medium [20]. In this context, adding Al<sub>2</sub>O<sub>3</sub> powder with nanoparticle size enlarges the machining gap distance between the electrode and workpiece. The insulating strength of the dielectric fluid decreases, as does the density of the energy. Which, in turn, generates a thinner white layer [21].

When comparing the results of this study to the results of [22], which concluded that during the machining of Inconel 718, the thickness of the white layer increased when the current increased from 20 to 70  $\mu$ m. Its formation had a significant effect on the mechanical properties of Inconel 718. This study achieved a lower WLT using a magnetic field with nano Al<sub>2</sub>O<sub>3</sub>.

According to Figure 5 and Table 3, it is clear that when applying current with higher values, more molten material will be generated, and more material will precipitate; thus, the thickness of the white layer increases. Similar to the effect of current,

an increase in pulse on time leads to an increase in white layer thickness because of the generation of high discharge energy in the machining zone. Also, the magnetic field causes an increase in white layer thickness. But when adding nano Al<sub>2</sub>O<sub>3</sub> to the insulating fluid, the WLT decreases at a concentration of 4 g/l as compared with no addition of it, and with the addition of nano Al<sub>2</sub>O<sub>3</sub> at a concentration of 2 g/l, due to the contribution of nano Al<sub>2</sub>O<sub>3</sub> particles in removing debris from the machining zone, thereby lowering the WLT obtained.

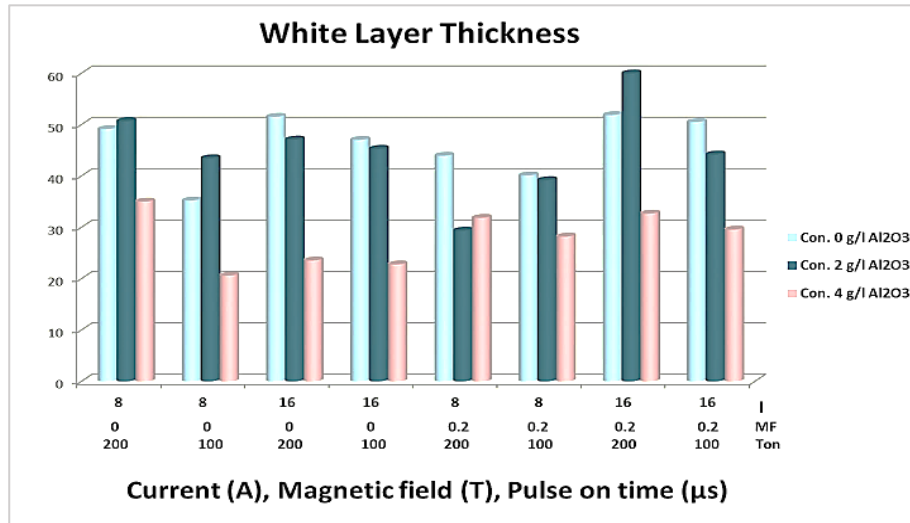


Figure 5: Parameters impact on WLT

Table 3: Average results of WLT and HAZ

Run	Current (A)	Ton (µs)	Con. (g/l)	MF (T)	Average WLT(µm)	Average HAZ(µm)
1	16	200	0	0.2	51.845	115.21
2	8	200	2	0.2	29.34	255.5
3	16	100	4	0.2	31.55	191.82
4	8	100	4	0	20.59	90.333
5	8	200	4	0	35	157.495
6	8	200	0	0	49.12	93.34
7	8	100	0	0	35.2	94.55
8	16	100	0	0.2	50.5	73.33
9	16	100	2	0.2	44.165	115.55
10	8	100	4	0.2	28.18	121.806
11	8	200	0	0.2	43.925	137.495
12	16	200	4	0	23.53	141.66
13	8	200	2	0	50.66	123.53
14	8	100	2	0	43.3	81.66
15	16	200	0	0	51.51	111.815
16	16	200	2	0.2	59.95	166.11
17	16	100	2	0	45.27	128.74
18	8	200	4	0.2	31.831	122.305
19	8	100	0	0.2	40.1	92.49
20	16	200	4	0.2	32.66	196.931
21	16	200	2	0	47.06	189.99
22	8	100	2	0.2	39.165	111.665
23	16	100	4	0	22.773	117.295
24	16	100	0	0	47.01667	103.0233

The minimum value for WLT was 20.59 µm; it was obtained at a concentration of 4 g/l, a current of 8 A, a pulse on time of 100 µs, and without using a magnetic field. The thickness of the white layer rose to 59.95 µm when the added powder was 2 g/l, the current was 16 A, the pulse on time was 200 µs, and the magnetic field intensity was 0.2 T. Figure 6 displays the microscopically taken pictures of the measured WLT and heat-affected zone HAZ. Figure 6a and b show the WLT of machined specimens without adding nano Al<sub>2</sub>O<sub>3</sub> and applying current with 16 and 8 A, respectively (runs 1 and 11). It is noticeable that the thickness of the white layer in Figure 6a is greater than Figure 6b due to the effect of current. Also, it is the same for Figure 6c and d, which machined by applying the parameters of runs 16 and 2, respectively, show that increasing current leads to an increase in WLT. Figure 6 e and f for machined specimens were obtained by applying the control parameters of runs 20 and 18 using 4 g/l of nano Al<sub>2</sub>O<sub>3</sub>, and it shows a thinner white layer as compared to other microscopically pictures.

Figure 7 represents the micrographs of the machined surface after adding 4 g/l of nano Al<sub>2</sub>O<sub>3</sub>, 16 A of applied current, 200 µs of applied pulse on time, and 0.2 T of magnetic field. The SEM micrographs revealed that the machined surface exhibits a

multifaceted appearance, as shown in Figure 7a. When using 1000x magnification in Figure 7b, the appearance of the machined surface becomes clearer and shows that it contains microcracks, voids, and globules of debris, and these are deemed surface defects, which reduce the surface quality and reduce fatigue and corrosion resistance of the produced surface. Therefore, adding nanopowders to the insulating fluid helps eliminate these defects.

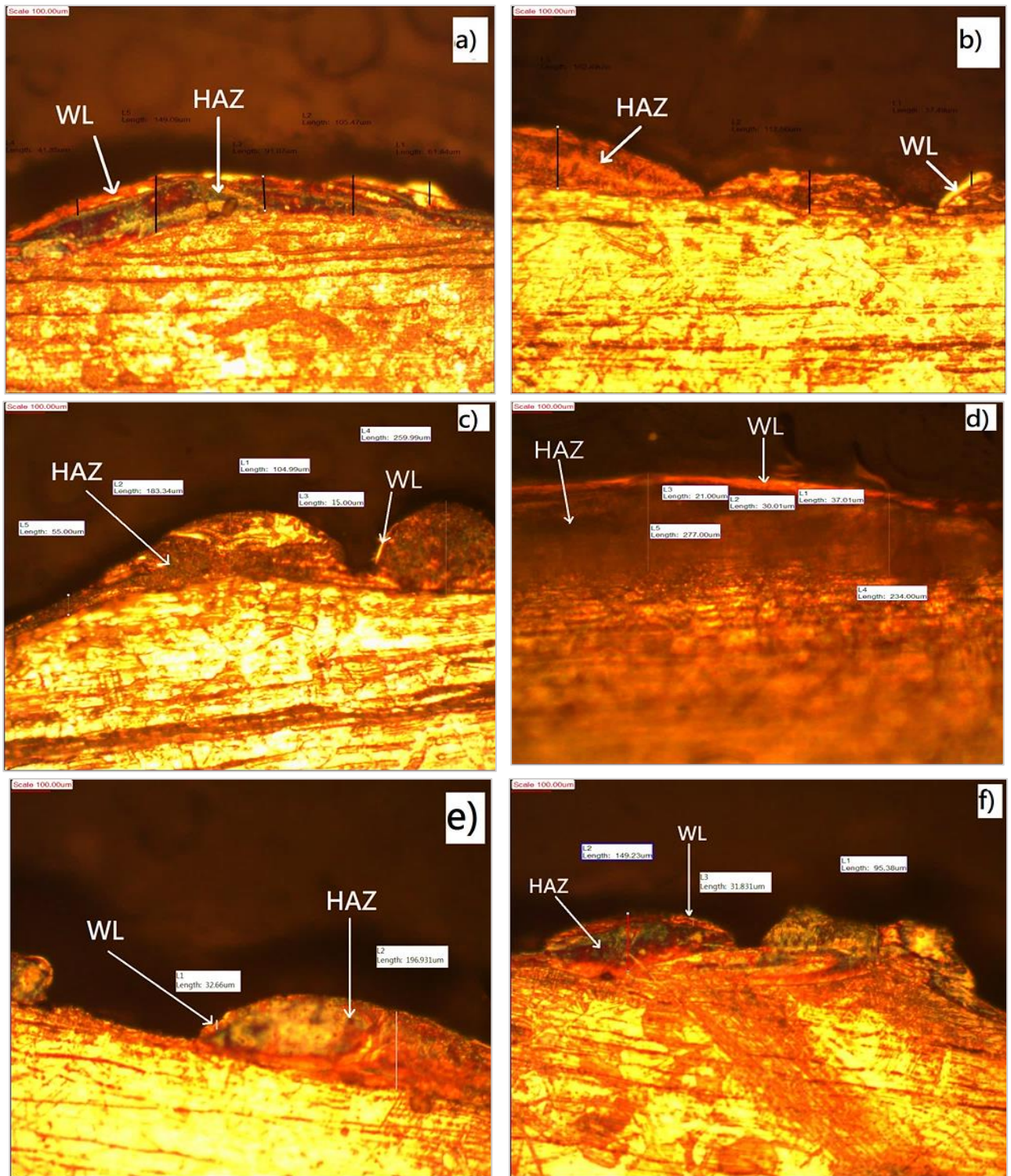


**Figure 6:** Microscopically pictures for measured WLT and HAZ a) I 16 A, Ton 200 µs, Con. 0 g/l, MF 0.2 T. b) I 8 A, Ton 200 µs, Con. 0 g/l, MF 0.2 T. c) I 16 A, Ton 200 µs, Con. 2 g/l, MF 0.2 T. d) I 8 A, Ton 200 µs, Con. 2 g/l, MF 0.2 T. e) I 16 A, Ton 200 µs, Con. 4 g/l, MF 0.2 T. f) I 8 A, Ton 200 µs, Con. 4 g/l, MF 0.2 T

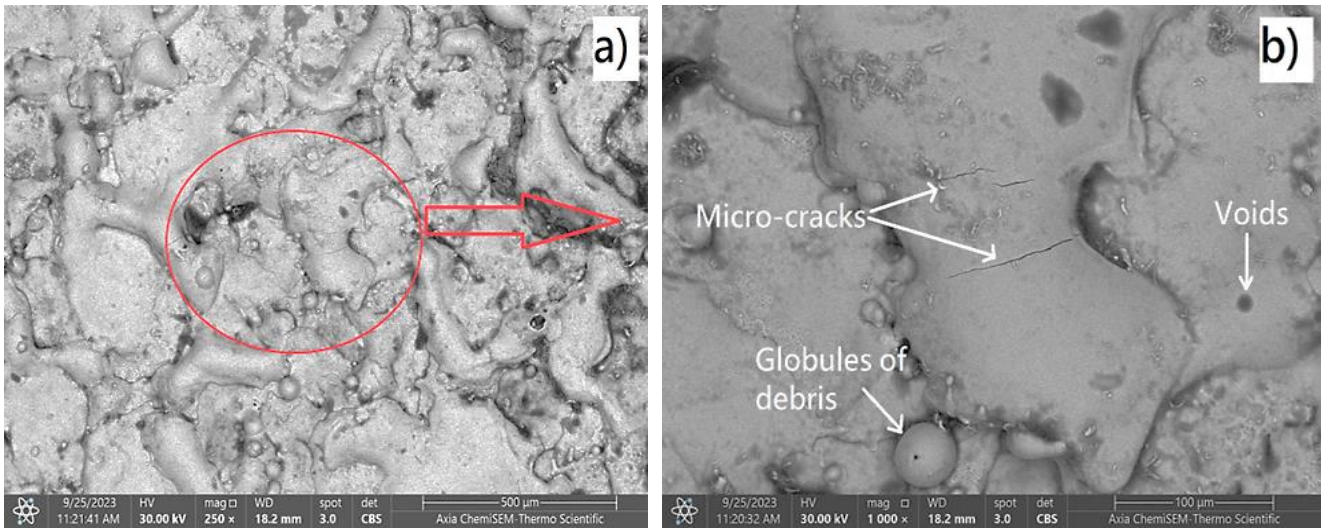


Figure 7: Micrographs of machined surface using 4 g/l of added nano- Al<sub>2</sub>O<sub>3</sub>, a) with 250x magnification b) with 1000x magnification

In light of Table 4, when analyzing the used factorial design of the results by Minitab, the analysis of variance results for measured WLT showed that the concentration of the added nano Al<sub>2</sub>O<sub>3</sub> has the most impact on WLT, followed by pulse on time and then the current.

Table 4: Analysis of variance for measured WLT

Source	Degrees of Freedom (DF)	Adj SS	Adj MS	F-Value	P-Value
Model	4	1939.0	484.76	13.48	0.000
Linear	4	1939.0	484.76	13.48	0.000
I	1	147.1	147.11	4.09	0.057
Ton	1	153.1	153.12	4.26	0.053
Con.	2	1638.8	819.40	22.78	0.000
Error	19	683.5	35.97		
Total	23	2622.5			

### 3.2 Impact of machining parameters on MRR

MRR is a substantial technical index in the product's manufacturing process. In contrast, the production efficiency in the EDM process is highly dependent on the amount of metal removed per unit time, as the more significant the MRR, the greater the production efficiency [23]. Patel et al. [24], reported that at 9 A, MRR is low, and it is greater at 28 A, so the current has the greater effect on MRR, pulse on time has a minor effect on MRR; it is greater at 150 μs than 50 μs when machining Inconel 718 using aluminum powder. Experimental results of this study proved that, too, and found that the peak current is the most influential parameter on MRR; it is directly proportionate to MRR, and as peak current increases, MRR increases too, due to the increase in the amount of discharge energy that causes the machined metal to melt and vaporize, resulting in higher MRR.

On the other hand, powder addition to dielectric fluid significantly contributes to the enhancement of MRR, whereas the existence of powder particles in the dielectric fluid leads to an increase in the thermal conductivity of the fluid; also, the frequency of the sparks increases, too, which in turn produces more MRR. The resulting MRR-measured values for different parameter settings are shown in Table 5. The practical experiments showed a considerable increase in MRR when the current increased; MRR was high, especially when the current was 16 A due to the increase in discharge energy that causes the metal to melt and vaporize, as is clear in Figure 5. The maximum obtained MRR was 13.25897 mm<sup>3</sup>/min when the value of current was 16 A, pulse on time was 200 μs, and Al<sub>2</sub>O<sub>3</sub> powder concentration was 2 g/l without using a magnetic field.

Pulse on time also has a significant effect on MRR. Greater energy, longer duration, and intensity for spark when the pulse on time increases; this produces more thermal energy and more molten metal, thereby a higher MRR. Also, it is noticed in Figure 8 that when increasing powder concentration to 4 g/l and current to 16 A, the MRR slightly decreases. This is because of arcing (abnormal discharging), which makes the process unstable, and thus the MRR decreases. In contrast, increasing nano Al<sub>2</sub>O<sub>3</sub> from 2 g/l to 4 g/l with a current value of 8 A leads to an increase in MRR without arcing. Based on Table 6, when analyzing experimental results using a general full factorial multi-level design by Minitab, the analysis of variance (ANOVA) showed that the design is statistically significant where the P values were less than (0.05). It is noticed that the current is the most influential factor, followed by the pulse on time, nano Al<sub>2</sub>O<sub>3</sub> powder concentration, and the magnetic field.

**Table 5:** Results of MRR and TWR according to design of experiments

Run	Current (A)	Ton( $\mu$ s)	Con. (g/l)	MF(T)	MRR ( $\text{mm}^3/\text{min}$ )	TWR ( $\text{mm}^3/\text{min}$ )
1	16	200	0	0.2	9.032521436	0.029841482
2	8	200	2	0.2	3.839703787	0.072253
3	16	100	4	0.2	9.500428854	0.093341
4	8	100	4	0	3.232334196	0.025271
5	8	200	4	0	3.8278231	0.073201
6	8	200	0	0	3.765869611	0.127602369
7	8	100	0	0	3.018369412	0.098323069
8	16	100	0	0.2	8.838800276	0.468474427
9	16	100	2	0.2	10.05415587	0.229515
10	8	100	4	0.2	3.32724231	0.022839
11	8	200	0	0.2	3.282078341	0.122571329
12	16	200	4	0	12.80950336	0.123643
13	8	200	2	0	3.689480065	0.034999
14	8	100	2	0	3.171689432	0.019448
15	16	200	0	0	11.03911783	0.282364854
16	16	200	2	0.2	12.84355935	0.260188
17	16	100	2	0	10.89520177	0.08647
18	8	200	4	0.2	5.056414293	0.034467
19	8	100	0	0.2	3.03030303	0.106026786
20	16	200	4	0.2	10.74209246	0.078125
21	16	200	2	0	13.25897373	0.097534
22	8	100	2	0.2	3.242963896	0.055287
23	16	100	4	0	10.63899604	0.101461
24	16	100	0	0	10.40125998	0.420513222

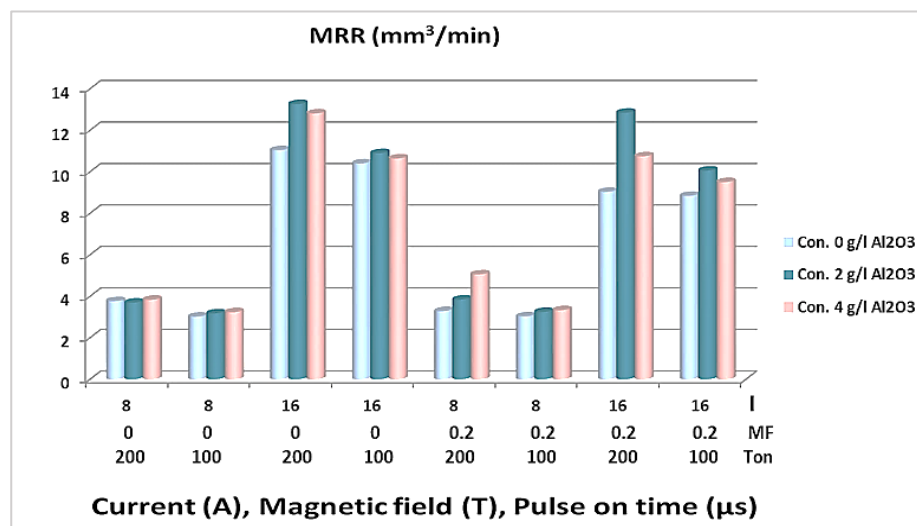


**Figure 8:** Parameters' impact on MRR

**Table 6:** Analysis of variance for MRR

Source	DF	Adj SS	Adj MS	F-Value	P-Value
Model	13	344.867	26.528	141.27	0.000
Linear	5	334.619	66.924	356.39	0.000
I	1	319.524	319.524	1701.54	0.000
Ton	1	7.976	7.976	42.47	0.000
Con.	2	5.102	2.551	13.59	0.001
MF	1	2.017	2.017	10.74	0.008
2-Way Interactions	6	9.082	1.514	8.06	0.002
I*Ton	1	1.024	1.024	5.46	0.042
I*Con.	2	3.136	1.568	8.35	0.007
I*MF	1	3.454	3.454	18.39	0.002
Ton*Con.	2	1.468	0.734	3.91	0.056
3-Way Interactions	2	1.166	0.583	3.10	0.089
I*Ton*Con.	2	1.166	0.583	3.10	0.089
Error	10	1.878	0.188		
Total	23	346.745			



### 3.3 Impact of machining parameters on tool wear rate

The accuracy of the machined parts relies on the accuracy of the tool's dimensions. The tool's mechanical, thermal, and physical properties affect the tool's wear rate. Electrode erosion is directly correlated with the erosion rate of the machined metal; the higher the eroded material, the greater the erosion ratio of the electrode [25]. TWR refers to the amount of material eroded from the electrode per minute. A copper electrode was selected due to its high melting point and high thermal conductivity, which help the heat quickly dissipate via the electrode, lessening the TWR. Compared to the results of [26], which reported that the lowest electrode wear rate EWR value of 0.244 mm<sup>3</sup>/min was achieved at the highest powder concentration of 4 g/l with the highest peak current of 40A and the longest pulse duration of 400 μs, the experimental results of this study achieved a lower value for TWR. The impacts of various parameters on TWR are shown in Figure 9. Current and pulse-on-time increments lead to higher TWR due to higher discharge, which causes greater heat at the machining zone, hence the higher TWR produced. The addition of nano Al<sub>2</sub>O<sub>3</sub> powder to the insulating fluid has a positive impact by reducing TWR, whereas the addition of it causes the machining gap to enlarge and the flushing mode to be enhanced; therefore, the TWR is lower; moreover, powder particles help in heat dissipation. Thus, the TWR is lessened. The higher powder concentration of nano Al<sub>2</sub>O<sub>3</sub>, the lowest TWR due to the increase in gap distance between the workpiece and the electrode, improves the flushing mode and makes the process more stable. On the other hand, using a magnetic field contributed to reducing TWR. Experimental results, which are displayed in Table 5, indicate that the minimum TWR was 0.022839 mm<sup>3</sup>/min when the current was 8 A, pulse on time 100 μs, nano Al<sub>2</sub>O<sub>3</sub> concentration 4 g/l and magnetic field intensity 0.2 T.

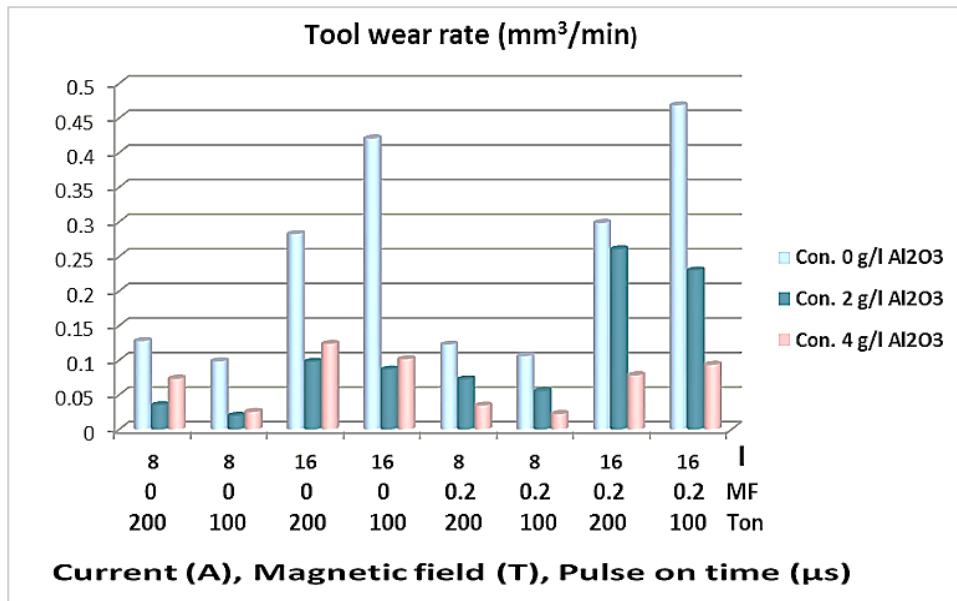


Figure 9: Impact of machining parameters on TWR

## 4. Conclusion

The current research studied the NPMEDM process to enhance its performance. The parameters, namely the concentration of nano Al<sub>2</sub>O<sub>3</sub>, current, pulse on time, and magnetic field, were optimized to obtain the best results for WLT, TWR, and MRR of NPMEDM. The findings led to the following conclusions:

- 1) Adding nano Al<sub>2</sub>O<sub>3</sub> produced better performance in terms of WLT, MRR, and TWR as responses.
- 2) An increment in current and pulse on time has a negative effect on WLT and TWR, where it leads to an increase in their values.
- 3) Increasing current and pulse-on-time values have a positive effect on MRR.
- 4) The magnetic field causes a slight increase in WLT, and when using it with a lower applied current 8 A, it leads to an increase in MRR. Also, the magnetic field positively affects TWR by reducing it.
- 5) The lowest WLT was achieved at a concentration of nano Al<sub>2</sub>O<sub>3</sub> 4 g/l, a current of 8 A, a pulse on time of 100 μs, and without using a magnetic field, which was 20.59 μm.
- 6) The maximum MRR obtained was 13.25897373 mm<sup>3</sup>/min at the highest level of current and pulse on time 16 A and 200 μs, respectively, and nano Al<sub>2</sub>O<sub>3</sub> powder concentration was 2 g/l without using a magnetic field.
- 7) The results of this study suggested that the minimum TWR was 0.022839 mm<sup>3</sup>/min when the current was the lowest 8 A, the pulse on time was the lowest 100 μs, the nano Al<sub>2</sub>O<sub>3</sub> concentration was the highest 4 g/l, and the magnetic field had an intensity 0.2 T.

The mechanisms of nanopowder mixed EDM remain insufficiently comprehended because they are affected by thermal, electrical, and chemical processes; therefore, it is required that they be thoughtfully investigated. Besides, there are still some challenges in changing the phase of the added powders due to the elevated temperature produced during the machining process and the development of microcracks and stresses on the machine surface. These aspects need closer examination in future studies.

## Abbreviations

Abbreviation	Meaning
NPEDM	Nano powder mixed electro-discharge machining process.
Al <sub>2</sub> O <sub>3</sub>	Aluminum oxide
MRR	Material removal rate (mm <sup>3</sup> /min)
WLT	White layer thickness (μm)
HAZ	Heat-affected zone (μm)
TWR	Tool wear rate (mm <sup>3</sup> /min)
EWR	Electrode wear rate (mm <sup>3</sup> /min)
I	Current (A)
Con.	Powder concentration (g/l)
MF	Magnetic field intensity (tesla)
Ton	Pulse on time (μs)
DF	Degrees of freedom

## Author contributions

Conceptualization, D. Ghulam and A. Ibrahim; Data curation, D. Ghulam.; formal analysis, D. Ghulam.; investigation, D. Ghulam.; Methodology, D. Ghulam and A. Ibrahim; Project administration, A. Ibrahim; Resources, D. Ghulam and A. Ibrahim; software, D. Ghulam.; supervision, A. Ibrahim.; Validation, D. Ghulam and A. Ibrahim; Visualization, D. Ghulam and A. Ibrahim; Writing - original draft, A. Ibrahim Supervision, D. Ghulam and A. Ibrahim; writing—review and editing, D. Ghulam and A. Ibrahim. All authors have read and agreed to the published version of the manuscript.

## Funding

This research received no specific grant from any funding agency in the public, commercial, or not-for-profit sectors.

## Data availability statement

The data supporting this study's findings are available on request from the corresponding author.

## Conflicts of interest

The authors declare that there is no conflict of interest.

## References

- [1] T.R. Ablyaz, E.S. Shlykov, K.R. Muratov, A. Mahajan, G. Singh, S. Devgan, S.S. Sidhu, Surface characterization and tribological performance analysis of electric discharge machined duplex stainless steel, *Micromachines*, 11 (2020) 2-14. <https://doi.org/10.3390/mi11100926>
- [2] X. Zhu, G. Li, J. Mo, S. Ding, Electrical discharge machining of semiconductor materials: A review, *J. Mater. Res. Technol.*, 25 (2023) 4354 – 4379. <https://doi.org/10.1016/j.jmrt.2023.06.202>
- [3] A. Goyal, A. Pandey, H. Rahman, Present and future prospective of shape memory alloys during machining by EDM/wire EDM process: a review, *Sadhana*, 47 (2022) 217. <https://doi.org/10.1007/s12046-022-01999-9>
- [4] A. Abdulwahhab, A. Ibrahim, Improvement of Performance Evaluation Using Hybrid Composite Electrode (Cu/Cr/WC/Ag) in Electric Discharge Machining, *Eng. Technol. J.*, 41 (2023) 1528-1538. <https://doi.org/10.30684/etj.2023.142962.1550>
- [5] T. Jadam, S. Sahu, S. Datta, M. Masanta, EDM performance of Inconel 718 superalloy: application of multi-walled carbon nanotube (MWCNT) added dielectric media, *J. Brazilian Soc. Mech. Sci. Eng.*, 41 (2019) 305. <https://doi.org/10.1007/s40430-019-1813-9>
- [6] A. Tiwary, B. Pradhan, B. Bhattacharyya, Influence of various metal powder mixed dielectric on micro-EDM characteristics of Ti-6Al-4V, *Mater. Manuf. Process.*, 34 (2019) 1103–1119. <https://doi.org/10.1080/10426914.2019.1628265>
- [7] A. Bhattacharya, A. Batish, N. Kumar, Surface characterization and material migration during surface modification of die steels with silicon, graphite and tungsten powder in EDM process, *J. Mech. Sci. Technol.*, 27 (2013) 133–140. <https://doi.org/10.1007/s12206-012-0883-8>
- [8] M. Mughal et al., Surface modification for osseointegration of Ti6Al4V ELI using powder mixed sinking EDM, *J. Mech. Behav. Biomed. Mater.*, 113 (2021) 104145. <https://doi.org/10.1016/j.jmbbm.2020.104145>
- [9] M. U. Farooq, M. P. Mughal, N. Ahmed, On the investigation of surface integrity of Ti6Al4V ELI using si-mixed electric discharge machining, *Materials*, 13 (2020) 1549. <https://doi.org/10.3390/ma13071549>

- [10] A. Ibrahim, Influence of electrical discharge machining parameters by additives Nano [AL<sub>2</sub>O<sub>3</sub>] on surface roughness and material removal rate in machining of AISI 304, *J. Phys. Conf. Ser.*, 1973 (2021) 012154. <https://doi.org/10.1088/1742-6596/1973/1/012154>
- [11] K. MangapathiRao, D. Vinaykumar, K.C. Shekar, R.R. Kumar, Investigation and analysis of EDM process – a new approach with Al<sub>2</sub>O<sub>3</sub> nano powder mixed in sunflower oil, *IOP Conf. Ser.: Mater. Sci. Eng.*, 1057,2021, 012059. <https://doi.org/10.1088/1757-899X/1057/1/012059>
- [12] M. Tawfiq , A. Hameed, Effect of Powder Concentration in PMEDM on Machining Performance for Different Die steel Types, *Eng. Technol. J.*, 33 (2015) 2174–2186. <http://dx.doi.org/10.30684/etj.2015.116235>
- [13] T. Jadam, S. Sahu, S. Datta, M. Masanta, Powder-mixed electro-discharge machining performance of Inconel 718 : effect of concentration of multi-walled carbon nanotube added to the dielectric media, *Sādhanā*, 45 (2020) 135. <http://dx.doi.org/10.1007/s12046-020-01378-2>
- [14] K. Paswan, A. Pramanik, S. Chattopadhyaya, Machining performance of Inconel 718 using graphene nanofluid in EDM, *Mater. Manuf. Process.*, 35 (2020) 33–42. <http://dx.doi.org/10.1080/10426914.2020.1711924>
- [15] A. Kumar, A. Mandal, A.R. Dixit, A.K. Das, S. Kumar, R. Ranjan, Comparison in the performance of EDM and NPMEDM using Al<sub>2</sub>O<sub>3</sub> nanopowder as an impurity in DI water dielectric, *Int. J. Adv. Manuf. Technol.*, 100 (2019) 1327–1339. <http://dx.doi.org/10.1007/s00170-018-3126-z>
- [16] A. Kumar, A. Mandal, A. Dixit, A. Das, Performance Evaluation of Al<sub>2</sub>O<sub>3</sub> Nano Powder Mixed Dielectric for Electric Discharge Machining of Inconel 825, *Mater. Manuf. Process.*, 33 (2017) 986-995. <http://dx.doi.org/10.1080/10426914.2017.1376081>
- [17] Z. Zhang, Y. Zhang, W. Ming, Y. Zhang, C. Cao, G. Zhang, A review on magnetic field assisted electrical discharge machining, *J. Manuf. Process.*, 64 (2021) 694–722. <http://dx.doi.org/10.1016/j.jmapro.2021.01.054>
- [18] M. Kolli , A. Kumar, Effect of dielectric fluid with surfactant and graphite powder on Electrical Discharge Machining of titanium alloy using Taguchi method, *Eng. Sci. Technol. Int. J.*, 18 (2015) 524-535. <http://dx.doi.org/10.1016/j.jestch.2015.03.009>
- [19] M. Ilani, M. Khoshnevisan, Study of surfactant effects on intermolecular forces ( IMF ) in powder-mixed electrical discharge machining ( EDM ) of Ti-6Al-4V, *Int. J. Adv. Manuf. Technol.*, 116 (2021) 1763–1782. <https://doi.org/10.1007/s00170-021-07569-3>
- [20] T. Muthuramalingam, Experimental Investigation of White Layer Formation on Machining Silicon Steel in PMEDM Process, *Silicon*, 13 (2021) 2257–2263. <https://doi.org/10.1007/s12633-020-00740-7>
- [21] R. Chaudhari, P. Prajapati, S. Khanna, J. Vora, V.K.Patel, D.Y. Pimenov, K. Giasin, Multi-Response Optimization of Al<sub>2</sub>O<sub>3</sub> Nanopowder-Mixed Wire Electrical Discharge Machining Process Parameters of Nitinol Shape Memory Alloy, *Materials*, 15 ( 2022) 2018. <https://doi.org/10.3390/ma15062018>
- [22] M. Xavior, N. Ranganathan, P. Ashwath, Effect of recast layer on the low cycle fatigue life of electric discharge machined inconel 718, *Mater. Today Proc.*, 5 (2018) 12666–12672. <https://doi.org/10.1016/j.matpr.2018.02.250>
- [23] W. Ming, Z. Xie, C. Cao, M. Liu, F. Zhang, Y. Yang, Research on EDM Performance of Renewable Dielectrics under Different Electrodes for Machining SKD11, *Crystals*, 12 (2022) 3-21. <https://doi.org/10.3390/cryst12020291>
- [24] S. Patel, D. Thesiya, A. Rajurkar, Aluminium powder mixed rotary electric discharge machining ( PMEDM ) on Inconel 718, *Aust. J. Mech. Eng.*, 16 (2017) 21-30. <https://doi.org/10.1080/14484846.2017.1294230>
- [25] M. P. G. Chandrashekarappa, S. Kumar, D.Y. Pimenov, K. Giasin, Experimental Analysis and Optimization of EDM Parameters on HcHcr Steel in Context with Different Electrodes and Dielectric Fluids Using Hybrid Taguchi-Based PCA-Utility and CRITIC-Utility Approaches, *Metals*, 11 (2021)1-22. <https://doi.org/10.3390/met11030419>
- [26] M. Lajis , S. Ahmad, Machinability performance of powder mixed dielectric in electrical discharge machining (EDM) of inconel 718 with copper electrode, *Int. J. Mech. Eng.*, 15 (2015).